

# SMBH mass determination in AGN from viscosity-correlated jet periodicities

P. Cassaro\*, R. A. Zappalà†, G. Palazzo†, G. Belvedere† and G. Lanzafame\*\*

\**Istituto di Radioastronomia INAF, Ctr.da Renna Bassa, 96017 Noto (SR), ITALY*

†*Dipartimento di Fisica e Astronomia, Università di Catania, via S. Sofia 78, 95123 Catania, ITALY*

\*\**Osservatorio Astrofisico di Catania, via S. Sofia 78, 95123 Catania, ITALY*

**Abstract.** Adopting the Smoothed Particle Hydrodynamics (SPH) numerical method we performed a time evolving model of a 3D axially symmetric viscous accretion disc around a Supermassive Black Hole (SMBH) of  $10^6 \div 10^9 M_\odot$ . The Shakura and Sunyaev standard viscosity  $\alpha$  prescription has been adopted. We find a link between viscosity and disc outflows for  $\alpha$  in the range between  $1.5 \cdot 10^{-3}$  and  $3 \cdot 10^{-3}$ , where both periodic and non-periodic outflows occur. These results could give an explanation for the origin of jets and refuelling in Active Galactic Nuclei (AGN). Moreover we are able to estimate the central SMBH mass by comparison of the model variability periods with the observed ones in the radio light curves of AGN.

**Keywords:** Accretion disks - Jets, outflows and bipolar flows - Quasars; active or peculiar galaxies, objects, and systems

**PACS:**

## INTRODUCTION

Collimated structures of outflowing plasma (jets) are observed in many classes of astrophysical objects: young stellar objects [26], X-ray binaries [18], planetary nebula nuclei [16], AGN [8, 3]. In particular, in AGN, jets frequently show non-continuous structures characterized by blobs of emission. The production of such blobs is connected with flares in the strongly variable light curves [22]. Generally the radio light curves of AGN do not exhibit any periodicity, but the analysis of the most time-extended radio light curves of some X and  $\gamma$  ray-loud blazars [33, 24] show the signature of a long-term quasi-periodic behaviour. Some of the observed periodic variabilities may be explained by the helical-jet model [12, 4, 23, 10, 27], but kinematic studies of parsec-scale radio jets have provided observational evidence for helical trajectories only in a few AGN showing periodicities [35, 30, 9, 11].

Direct observations show that accretion discs are a common feature for all jet-producing systems. It is widely accepted that the mechanism of mass loss through outflows and jets from the disc is directly linked to accretion processes. According to some hydromagnetic mechanisms [2, 15, 32] magnetic fields provide a mechanical connection between jets and discs to explain jet production, confinement and collimation. But fundamental questions remain unresolved about the origin of magnetic fields and their geometry. In this paper, we present a model where outflows and jet formation are intimately related to accretion disc physical viscosity, by using a purely fluid dynamics numerical code without taking into account the magnetic fields role.

## MODEL DESCRIPTION

In the SPH framework [17, 20] we carried out an accretion disc model around a SMBH ( $M_{SMBH} = 10^6 \div 10^9 M_\odot$ ) in axisymmetric conditions following Lanzafame et al. [14] in cylindrical coordinates, assuming all the derivatives  $d/d\phi$  equal to zero. We model the non-rotating central compact object using the pseudo-Newtonian potential proposed by Paczynski & Wiita [21]:

$$\Phi = -\frac{1}{2(R-1)} \quad (1)$$

where  $R = r\hat{r} + z\hat{z}$  is the radial distance.  $r$  and  $z$ , as well as the other lengths are in units of Schwarzschild radius. The inclusion of viscosity in the form of Shakura-Sunyaev prescription [28, 29] implies that the specific angular momentum  $\lambda$  is not constant everywhere. Rather, it is transported outwards at a rate determined by viscosity.

We set the injection of the particles at 30 Schwarzschild radii ( $R_g$ ). Time, velocity, angular momentum and energy have scale factors of  $2GM_{SMBH}/c^3$ ,  $c$ ,  $2GM_{SMBH}/c$  and  $c^2$ , respectively. All the quantities present in this simulation, if

involving the mass, are to be considered per unit mass. The SPH resolution is  $h = 0.3$ . We set the initial values of radial velocity  $v_r$  and specific angular momentum  $\lambda$  of injected particles as  $v_r=0.1$  and  $\lambda=1.6$ . The initial specific thermal energy is  $U_{th} = 1.08 \cdot 10^{-2}$ . We chose these values in order to have the initial total energy of the particles equal to zero, accordingly with the total energy calculation reported in Molteni et al. [19]. At  $1 R_g$  the particles are eliminated, simulating the downfall onto the black hole. Of course the values of all physical quantities in the disc vary with radial distance and time.

## RESULTS

In Lanzafame et al. [14] a similar simulation has been carried out with  $0 \leq \alpha \leq 1.5 \cdot 10^{-3}$ , relating the Shakura-Sunyaev viscosity to an outflow, due to the impact of the accreting mass with a shock front, with intensity growing with the viscosity parameter. In that model it has been observed a periodic oscillation of the outflow for  $\alpha = 1.5 \cdot 10^{-3}$ , correlated to the presence of an oscillation of the shock front. The shock front develops, drives away from the SMBH, smooths out, and then restores.

The simulation has been repeated, with the viscosity parameter equal to  $2.0 \cdot 10^{-3}$ ,  $2.5 \cdot 10^{-3}$  and  $3.0 \cdot 10^{-3}$ , and this is object of the present work. Let us examine the results using the first two values. In such cases the outflow is still present and it oscillates in the same way as with  $\alpha = 1.5 \cdot 10^{-3}$ . An example of this, with  $\alpha = 2 \cdot 10^{-3}$ ,  $v_r=0.1c$  and  $\lambda=1.6$ , is reported in Fig. 1. In this figure four phases, from a) to d), of the oscillation of the shock front are reported. For each phase are plotted, in the first plot of each column the positions of the SPH particles. The other plots are the radial mach number, the angular momentum, the density and the thermal energy at the equatorial plane, versus the radius. The radius is expressed in Schwarzschild radius units, while the angular momentum is, as reported in the previous section, in units of  $2GM_{SMBH}/c$  and the thermal energy is in units of  $c^2$ . We stress that all these quantities are per unit mass. At the top of each column of the plots, the number of particles for each phase is reported. The particle number in each simulation varies in time from about 6000 to about 14000, following an oscillating behaviour.

In the phase a), the shock front is at its maximum distance from the SMBH ( $12 R_s$ ). The accreting matter has piled up on the shock front and the accretion rate is at its minimum. In the phase b) the matter is driven out from the plan of the disc and the shock front begins to disrupt. In the phase c) the shock front has been disrupted and the outflow is not fuelled anymore slowing down rapidly. The matter falls down more or less directly towards the SMBH and the accretion rate grows up. In the phase d) the shock front comes back at a distance of about  $6 R_s$ . It will be driven out because other accreting matter will pile up on the shock front again, reporting the system to the phase a).

In Fig. 2 the mass loss through the outflows is showed versus time for three different values of the viscosity parameter. For  $\alpha$  equal to  $2.0 \cdot 10^{-3}$  and  $2.5 \cdot 10^{-3}$  we observe a step-like behaviour, corresponding to phases outflowing alternated to phases without outflow. The outflow period is:

$$T = \tau \cdot \frac{2GM_{SMBH}}{c^3} = t \cdot M_{SMBH} \text{ (sec)} \quad (2)$$

where  $t = \frac{2GM_{SMBH}}{c^3}$  is the time in the units of the simulation and the MKS system was adopted. Therefore, the more massive is the object, the longer is the period. In our simulations  $t = (1.60 \pm 0.25) \cdot 10^{-32}$  for  $\alpha = 2 \cdot 10^{-3}$ , and  $t = (2.25 \pm 0.25) \cdot 10^{-32}$  for  $\alpha = 2.5 \cdot 10^{-3}$ , showing the weak dependence of the period from the Shakura-Sunyaev viscosity parameter. When we select a value for the mass of the SMBH, the period is converted into seconds. In Tab. 1 the values of the period for  $10^6 M_\odot < M_{SMBH} < 10^9 M_\odot$  are reported.

## DISCUSSION AND CONCLUSIONS

The simulations we have carried out and the previous results of Lanzafame et al. [14], lead to an important role of the viscosity parameter on the production and modulation of the outflows in Active Galactic Nuclei (AGN). Increasing the viscosity the outflow is initially enhanced, then it becomes periodical, and finally it increases more strongly losing the periodical behaviour.

When the viscosity parameter ranges from 0 to  $1.0 \cdot 10^{-3}$ , the angular momentum begins to be transferred outwards from the inner regions of the disc.

In Fig. 3 the disc mass is showed versus time for three different values of the viscosity parameter. It is easy to observe that there is an anticorrelation between the disc mass and the outflow: we do not observe outflows during the increase of the disc mass.

**TABLE 1.** Oscillation periods as function of the SMBH masses and of the viscosity parameter: col. [1] SMBH mass in solar mass units, col. [2] corresponding outflow period for  $\alpha = 2.0 \cdot 10^{-3}$  and, col. [3] for  $\alpha = 2.5 \cdot 10^{-3}$ . It is evident the strong dependence from the SMBH mass.

[1]	[2]	[3]
$M_{SMBH}$ ( $M_{\odot}$ )	$T_{\alpha 1}$ (sec)	$T_{\alpha 2}$ (sec)
$10^6$	$3.2 \pm 0.5 \cdot 10^4$	$4.5 \pm 0.5 \cdot 10^4$
$10^7$	$3.2 \pm 0.5 \cdot 10^5$	$4.5 \pm 0.5 \cdot 10^5$
$10^8$	$3.2 \pm 0.5 \cdot 10^6$	$4.5 \pm 0.5 \cdot 10^6$
$10^9$	$3.2 \pm 0.5 \cdot 10^7$	$4.5 \pm 0.5 \cdot 10^7$

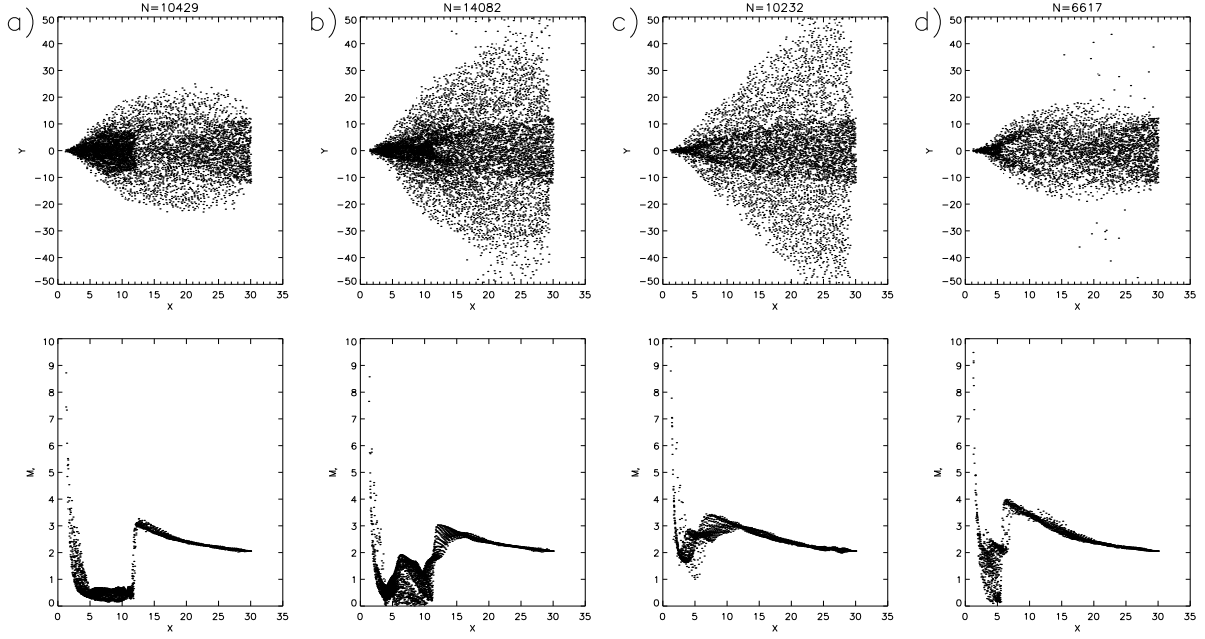


**FIGURE 1.** Four phases of the simulation with  $\alpha = 2 \cdot 10^{-3}$ ,  $v_r=0.1c$  and  $\lambda=1.6$ . The first plot of each column represents the positions of the SPH particles. Here about one half of the particles are represented, to make the plots more readable. The second plot reports the radial Mach number versus the radial distance, expressed in units of the Schwartzschild radius, for the equatorial plane of the disc. At the top of each column, the total number of particles for that phase is reported. Time increases from a) to d). See the text for details.

The oscillation of the shock front disappears when higher viscosity parameters are considered. We performed a simulation with  $\alpha = 3.0 \cdot 10^{-3}$ , and the results are summarized in Figs. 2 and 3. In Fig. 2 the outflow for  $\alpha = 3.0 \cdot 10^{-3}$  is shows no oscillations. In Fig. 3, for the same  $\alpha$  value, a very weak oscillation of the disc mass can be recognized, very hard to observe, anyway.

In this way a shock front is built, and the matter coming from the outer disc regions is partially deflected out, creating a thin outflow. For viscous disc models whose  $\alpha$  ranges from the  $\alpha = 1.5 \cdot 10^{-3}$  to  $\alpha \sim 2.5 \cdot 10^{-3}$ , an oscillating behaviour, illustrated in Fig. 1 appears. It is possible to explain such behaviour considering that in the inner part of the disc the angular momentum is transferred outwards, as it can be seen in the phase a) of Fig. 1. The shock front is formed at higher distance from the SMBH the higher is the viscosity parameter. The matter accreting from the outer region loses angular momentum more efficiently, reaching the shock front, where a fraction of the incoming matter is expelled from the disc plane while the rest begins to piles up on the shock front at a rate higher than that of the matter that leaves it on the other side of the shock front. When the density in the region beyond the shock front has reached

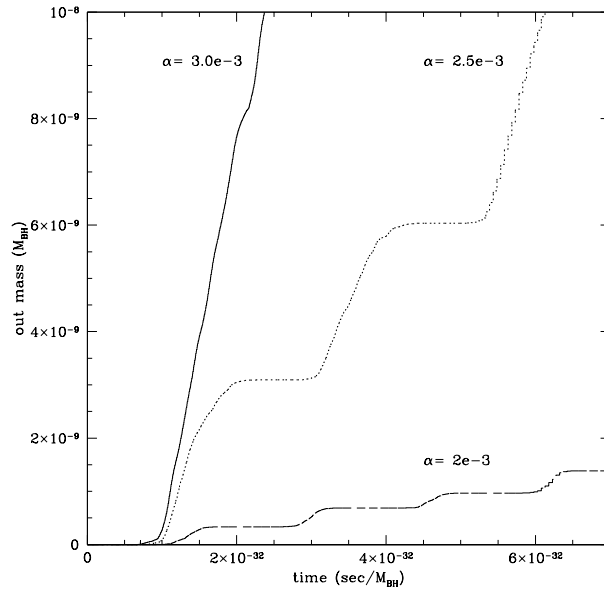


**FIGURE 2.** The mass loss through the outflows is showed versus time for three different values of the viscosity parameter:  $\alpha = 2 \cdot 10^{-3}$  (dashed line),  $\alpha = 2.5 \cdot 10^{-3}$  (dotted line),  $\alpha = 3 \cdot 10^{-3}$  (continuous line). Here, time is in the units of the simulation. By multiplying by the SMBH mass, we get time in seconds.

a critical value (see Fig. 1, phases a and b), the interactions between the particles become more important leading to a quick loss of angular momentum in this region. The transfer of angular momentum from the inner part of the disc cannot sustain the shock front. Therefore the shock front degrades suddenly. It can be seen from the other phases in Fig. 1 that the angular momentum drops down, after the shock front disruption, from the shock front region inwards, as well as the density. After some time the shock front restores and the process described restarts. When  $\alpha = 3.0 \cdot 10^{-3}$  the oscillating behaviour falls down and the shock front becomes steady, with a steady outflow at higher rate than in the oscillating regime. This occurs because the rates of the piling up and the removal of the matter on the two sides of the shock front become almost the same, and the outflow loses the oscillatory behaviour.

The outflow of our model can be correlated to the synchrotron radio emission because the ejected gas will be channeled and injected in the galactic magnetic field. In such a way the variation in the outflow from the disc surface is related to variations in the radio emission. Such a behaviour is consistent with the radio structure observed in high resolution images of radio loud AGN, where are visible blobbed structures, that can be related to the pulsating ejection of matter from the disc surface. In low resolution images, the modulations of the gas ejection appears in a radio flux density variability, that has been observed in many objects. In particular there are several studies of radio light curves on single objects (e.g. Raiteri et al. [24], Vicente et al. [35]) or on group of blazars (e.g. Venturi et al. [33]). In these last works, it is possible to recognize a quasi periodical variability in the sources, much more evident in the high frequency light curves [31]. Extrapolating the variability periods  $T$  from the observed light curves of some blazars that exhibit a periodicity, we can estimate the central SMBH mass, inverting relation (2). In Tab. 2 the masses calculated with this method are reported for  $\alpha = 2.5 \times 10^{-3}$ . The light curves of the objects have been collected from Teräsranta et al. [31] and Venturi et al. [33]. The values calculated are in agreement with that obtained, for some of the sources, by other methods [13, 1, 5, 34, 37], that are reported in the same Table. The mass estimate are very weakly dependent on the  $\alpha$  value, being determining the dependence on the period.

Concluding in this work we considered the role of viscosity in order to parametrize a model of accretion disc. The results can be summarized as:

- the viscosity parameter is connected to the outflow production;
- the existence of values of the viscosity parameter that produce continuous mass loss from disc;
- the existence of a range of values of the viscosity parameter that produce periodic outflows;

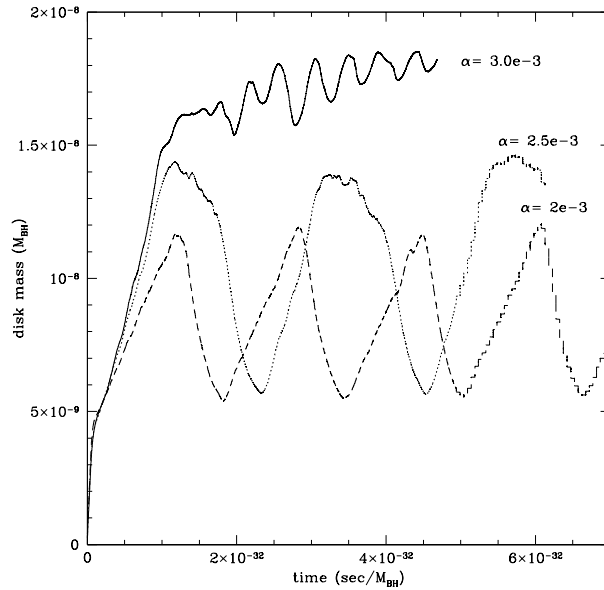


**FIGURE 3.** The disc mass is showed versus time for three different values of the viscosity parameter (the same as in Fig.2). Here, time is in the units of the simulation. By multiplying by the SMBH mass, we get time in seconds.

**TABLE 2.** Observed oscillation periods and SMBH masses: col. [1] name of the source, col. [2] variability period, col. [3] reference for the radio light curve: (1), Venturi et al. (2001), (2) Terasranta et al. (2005). Col.[4] black hole mass calculated for  $\alpha = 2.5 \cdot 10^{-3}$ , col.[5] black hole mass from the literature, col. [6] reference for col. [5]: (1) Cao 2003, (2) Barth et al. (2002), (3) Kotilainen et al. (2002)., (4) Vestergaard & Peterson (2006), (5) Xie et al. (2005)

[1]	[2]	[3]	[4]	[5]	[6]
Name	T ( $\cdot 10^7 s$ )	ref.	$M_{SMBH}$ ( $\cdot 10^9 M_{\odot}$ )	$M_{oth}$ ( $\cdot 10^9 M_{\odot}$ )	ref.
0235+164	$18.0 \pm 3.0$	1	$4.0 \pm 0.8$	$< 26.0$	1
1101+384	$5.6 \pm 2.2$	1	$1.2 \pm 0.5$	0.19	2
				0.45	3
1226+023	$6.1 \pm 1.8$	1	$1.4 \pm 0.4$	1.6	4
	$7.2 \pm 1.8$	2	$1.4 \pm 0.4$		
1418+546	$4.6 \pm 1.9$	1	$1.0 \pm 0.4$	1.1	1
1803+784	$4.3 \pm 1.6$	1	$0.9 \pm 0.4$	$< 1.3$	1
1807+698	$4.0 \pm 2.2$	1	$0.9 \pm 0.5$	0.32	2
				0.79	3
				1.0	1
2007+777	$4.2 \pm 2.2$	1	$0.9 \pm 0.5$	0.78	1
2251+158	$3.9 \pm 1.7$	2	$0.9 \pm 0.4$	1.4	5

- the possibility of determination of the SMBH mass from the kinematics of the outflows.

We believe that these preliminary results justify further investigations. Therefore, new simulations will be carried out for different values of the viscosity parameter versus different values of the radial velocity and specific angular momentum of the injected particles. In this context we want to estimate the thermal emission of the disc and the non-thermal emission of the outflows. It can be seen that the black holes of the sources considered in the literature have a mass  $> 10^8 M_{\odot}$ , corresponding to periods larger than one year. This because available radio light curves have a time resolution too wide as to correctly sample a shorter period, this leading to a smoothing of the periodicities,

unrecognizable at a visual inspection. Hence, further observation and analysis of sources at 22 and 43 Ghz are necessary in order to study the variability.

## REFERENCES

1. Barth, A.J., Ho, L.C., Sargent, W.L.W., 2003, ApJ, 583, 134
2. Blandford, R.D., Payne, D.G., 1982, MNRAS, 199, 883
3. Bragg, A.E., Greenhill, L.J., Moran, J.M., Henkel, C., 2000, ApJ, 535, 73
4. Camenzind M., Krockenberg M., 1992, A&A, 255, 59
5. Cao, X., 2003, ApJ, 599, 147
6. Chakrabarti, S.K., 1989, ApJ, 347, 365
7. Chakrabarti, S.K., 1990, Theory of Transonic Astrophysical Flow (Singapore, World Scientific)
8. Ferrarese, L., Ford, H.C., 1999, ApJ, 515, 583
9. Gomez J., Marscher A.P., Alberdi A., Gabuzda D.C., 1999, ApJ, 519, 642
10. Guerra E.J., 2004, AAS Meeting 205, 178.04
11. Kellermann, K.I., Lister M.L., Homan D.C. et al., 2004, ApJ, 609, 539
12. Konigl, A., Choudhuri A. R., 1985, ApJ, 289, 173
13. Kotilainen, J.K., Falomo, R., Treves, A., 2002 in High energy blazar astronomy, ASP Conference Series 299, eds Takolo, L.O., Valtaoja, E.
14. Lanzafame, G., Molteni, D., Chakrabarti, S.K., 1998, MNRAS 299, 799
15. Li, Z., Chiueh, T., Begelman, M.C., 1992, ApJ, 394, 459
16. Lopez, J.A., 1997, IAU Symposium N. 180
17. Lucy, L., 1977, AJ, 82, 1013
18. Mirabel, I.F., Rodriguez, L.F., 1999, ARA&A, 37, 409
19. Molteni, D., Lanzafame, G., Chakrabarti, S. K., 1994, ApJ, 425, 161
20. Monaghan, J.J., 1992, ARA&A, 30, 543
21. Paczynski B., Wiita P.J., 1980, A&A, 88, 23
22. Perlman, E.S., Biretta, J.A., Sparks, W.B., et al., 2001, ApJ, 551, 206
23. Raiteri C.M., Villata M., Tosti G., et al., 1999, A&A, 352, 19
24. Raiteri, C.M., Villata, M., Aller, H.D. et al., 2001, A&A, 377, 396
25. Raiteri, C.M., Villata, M., Ibrahimov, M. A., et al., 2005, A&A, 438, 39
26. Reipurth, B., Bertout, C., 1997, IAU Symposium N.182.
27. Rieger F.M., 2004, ApJ 615, L5
28. Shakura, N.I., 1972, Astron. Zh., 49, 921, (English tr.: 1973, Sov.Astron., 16, 756)
29. Shakura, N.I., Sunyaev R.A., 1973, A&A, 24, 337
30. Tateyama C.E., Kingham K.A., Kaufmann P. et al., 1998, ApJ, 500, 810
31. Teräsranta, H., Wiren, S., Koivisto, P., Saarinen, V., Hovatta, T., 2005, A&A, 440, 409
32. Tout, C.A., Pringle, J.E., 1996, MNRAS, 281, 219
33. Venturi, T., Dallacasa, D., Orfei, A., et al., 2001, A&A 379, 755
34. Vestergaard, M., Peterson, B.M., 2006, ApJ, 641, 689
35. Vicente L., Charlot P., Sol H., 1996, A&A, 312, 727
36. Villata, M., Raiteri, C. M., Aller, H. D., A&A, 424, 497
37. Xie, G.Z., Chen, L.E., Xie, Z.H., Ma, L., Zhou, S.B., 2005, PASJ, 57, 183